

Calculation of the Surface Photoelectric Effect

J. G. Endriz*

Department of Physics, University of Linköping, Linköping, Sweden

(Received 25 May 1972)

A modified form of the Mitchell-Makinson time-dependent perturbative calculation of the surface photoelectric effect has been carried out based on a significantly improved treatment of surface-polarization charge-density variations. The approach taken allows calculation of the excitation current back into the metal as well as into vacuum, and is generally applicable to the surface wave (plasmon) or to the direct optical mode of p -polarized-light excitation of the surface effect. Numerical results are presented for aluminum, but the general conclusions of the paper should be applicable to all nearly-free-electron metals. The behavior of the surface charge is shown to have a fundamental effect upon the frequency dependence of the surface effect, causing a marked enhancement in the effect at low energies followed by an almost total suppression of the surface effect at energies near the volume plasma energy. Surface photoexcitation at these lower energies is shown to dominate the photoemission from surface-wave decay as well as from direct optical excitation at high angles of light incidence. The surface-wave (plasmon) mode of excitation is shown to be particularly strong, with surface excitation dominating the decay of the high- k plasmons typically excited on real surfaces. Comparisons of the results of this calculation are made with existing experimental data, and the prediction that surface waves (plasmons) should form a uniquely strong mode of surface-effect excitation is shown to be quantitatively consistent with recent experimental studies of photoemission in surface-plasmon decay. The historical failure to observe direct optical excitation of the surface photoelectric effect in the alkalis is explained, and a suggestion for detecting direct-optical excitation of the effect in other nearly-free-electron metals is made based on the results of this calculation.

I. INTRODUCTION

Calculations of the surface photoelectric effect have a long history,¹⁻⁶ but have suffered over the years from inadequate treatments of the electromagnetic excitation fields. These inadequacies have arisen in part from the theoretical problem in treating the dynamic behavior of an electron gas near its surface, and in part from the opinion that experimentally obtainable metallic films could not be made atomically smooth. In the present paper new perspectives on these problems are presented as they relate to the macroscopic behavior of the excitation fields vs polarization, angle of incidence, and energy of excitation, and as they relate to the microscopic behavior of the fields at the surface. *Proper treatment of these effects are shown to have fundamental implications on the angular and frequency ranges over which the surface photoelectric effect can be expected to be observed.* Quantitative results are presented for the surface photoelectric effect in aluminum (Al), but the approach and many of the conclusions of this paper should be considered generally applicable to all nearly-free-electron metals.

Surface photoexcitation is by definition an excitation process in metals by which momentum is conserved via electronic reflection at the surface. It follows that this process can only occur if there is an excitation field component normal to the surface. Calculations of the surface photoeffect thus depend critically upon the detailed macroscopic

and microscopic behavior of this normal field component. The microscopic behavior of this field component near the surface is related to the dynamic behavior of surface-polarization charge fluctuations. In the present paper recent attempts to characterize these charge-density variations^{7,8} are applied for the first time to a surface-effect calculation. Of comparable importance is the shifted perspective of this paper concerning the macroscopic behavior of the excitation fields.

It has long been realized that the calculation and detection of the surface photoeffect would be greatly simplified if one could assume ideal or atomically smooth surfaces such that only oblique-incidence p -polarized light could couple to the effect. Unfortunately, the implications of this view have not been pursued in previous calculations owing to past experimental difficulties in obtaining atomically smooth and atomically clean metallic films. Several calculations have in fact been devoted to surface photoexcitation on roughened surfaces.³ Quite recent studies⁹⁻¹¹ of vacuum-evaporated films of various metals indicate that under proper preparation circumstances, films of certain metals can be prepared which are atomically smooth. Typical of these results is the striking transmission-electron micrograph of a 158-Å-thick evaporated-gold (Au) film taken by Théye⁹ and shown in Fig. 1. The micrograph indicates very flat, smooth crystallites with lateral dimensions comparable to a 1 μ , and having only slight depressions of a few angstroms along grain boundaries. While

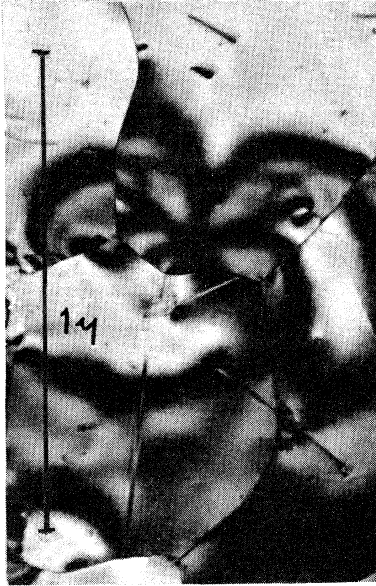


FIG. 1. Transmission electron micrograph of a 158-Å-thick vacuum-evaporated film of Au. Note that the lateral dimensions of the crystals are comparable to 1μ (M. L. Théye, Ref. 9).

Au is not a nearly-free-electron metal, films of other metals, including Al^{10,11} have indicated comparable structure.

Throughout the calculations of this paper it is assumed that such smooth metallic surfaces are indeed experimentally achievable. This assumption greatly simplifies the treatment of macroscopic variations in the excitation fields and allows a general calculation of the surface effect in terms of p -polarized-light excitation at an arbitrary angle of incidence. For such smooth surfaces, the important but spurious coupling to surface waves can be ignored. Surface-wave (plasmon) excitation, where it does occur, is treated as a special case of p -polarized-light excitation at an appropriate complex angle of incidence.¹²

Existing experimental evidence for the surface effect in plasmon decay^{11,13} and previous failures¹⁴⁻¹⁷ to unambiguously detect the surface effect in optical excitation are both discussed within the context of the present results. Implications of these calculations with regard to possible future detection of the surface effect are also described.

II. CALCULATION

The model used for the present calculation of surface photoelectric excitation is a modification of the time-dependent perturbative approach to the problem first taken by Mitchell.^{2,3} This model assumes that the metal is well approximated by a free-electron gas, and in the present calculation, we assume an image charge potential at the sur-

face. The all important divergence term in the excitation Hamiltonian is included as first suggested by Makinson,⁴ and the excitation fields in the region of the surface-polarization charge are derived based on the Bloch hydrodynamic equations. This latter contribution is shown to be of fundamental importance in accurately evaluating the strength and frequency dependence of the surface effect. A detailed treatment of the macroscopic field configurations of the exciting fields is simplified by assuming ideally smooth surfaces with all excitation via p -polarized light at oblique angles of incidence. The special case of surface-effect excitation by surface waves (plasmons) is analytically treated as excitation by p -polarized light at an appropriate *complex* angle of incidence after an approach first taken by Stratton.¹²

The Mitchell-Makinson model, as a perturbative theory, necessarily implies that excitation fields are unchanged by surface excitation. This criticism of the model, extensively dealt with in the present paper, has been specifically directed¹⁸ toward recent surface-plasmon-decay calculations,¹¹ although any criticisms of the theory must be equally applicable to optical modes of excitation. The strength of the present calculation lies in its unique treatment of field variations near the surface, an approach which any improved theory must include. The present approach is further strengthened by the agreement of Adawi's⁵ more sophisticated Green-function approach to the problem with the result of Mitchell's early theory.¹ As a final point, we note that the idealization implicit in assuming a completely free-electron gas necessarily excludes the type of interference effects between volume and surface photoexcitation first suggested by Schaich and Ashcroft,⁶ although Mahan¹⁹ has noted that these effects may be rather small.

A. Characteristic Photoexcitation

The calculations of this section include the determination of expressions for surface photoexcitation back into the volume of the metal, as well as surface-effect photoemission into vacuum. It is emphasized that the assumption of ideally smooth surfaces implies that the shape of the spacial variation in the normal component of the excitation field is independent of angle of incidence. This allows factorization of surface excitation into angular factors dependent upon energy, angle of light incidence, and optical constants, and factors termed characteristic photoexcitation, independent of angle of incidence. The formalism is equally applicable to optical excitation of the surface effect at real angles of incidence or surface-plasmon excitation at complex angles of incidence.

Beginning with the assumptions of the Mitchell-Makinson model, the form of the external photo-

current resulting from the excitation of a single electron within the Fermi sea can be shown to be

$$(j_z)_{\text{emitted}} = (4\pi^2 em/\hbar f) |\langle M_f \rangle|^2, \quad (1)$$

where $\hbar f$ is the z component (normal to the surface) of momentum for the final, photoemitted electron state. The matrix element $\langle M_f \rangle$, coupling the initial and final electron states in the excitation process is given by

$$\langle M_f \rangle = \frac{(e/mc)b_f}{2\pi|b_f|^2} \times \int_{-\infty}^{\infty} dz \left(\vec{a}_z \frac{\partial \psi_k}{\partial z} + \frac{1}{2} \psi_k \frac{\partial \vec{a}_z}{\partial z} \right) (\psi_f^{*} - a_f^* \psi_f^{-*}). \quad (2)$$

Following the approach and notation of Mitchell,² the initial-state wave function in the excitation is given by

$$\begin{aligned} \psi_k &= e^{-iI(z-z_0)} + a_k e^{iI(z-z_0)}, \quad z < z_0 \\ &= b_k W_{s/k, 1/2}(2kz), \quad z > z_0 \end{aligned} \quad (3)$$

and the final-state wave functions are given by

$$\begin{aligned} \psi_f^+ &= e^{-iG(z-z_0)} + a_f e^{iG(z-z_0)}, \quad z < z_0 \\ &= b_f W_{-is/f, 1/2}(2ifz), \quad z > z_0 \end{aligned} \quad (4a)$$

$$\begin{aligned} \psi_f^- &= a_f^* e^{-iG(z-z_0)} + e^{iG(z-z_0)}, \quad z < z_0 \\ &= b_f^* [W_{-is/f, 1/2}(2ifz)]^*, \quad z > z_0. \end{aligned} \quad (4b)$$

ψ^+ and ψ^- relate to whether the excited wave function is outgoing or incoming at large distances on the vacuum side of the metallic surface, $W_{\alpha, 1/2}(\chi)$ is a confluent hypergeometric function,²⁰ the solution to the unperturbed wave equation in the region of the image potential

$$V = -e^2/4z, \quad z > z_0. \quad (5)$$

For $z < z_0$, the potential is a constant, $V_0 \equiv -e^2/4z_0$. The parameter s in Eqs. (3) and (4) is given by $s = \pi^2 m e^2 / \hbar^2$.

In the above expressions for initial- and final-state wave functions, the electron momenta are given by

$$\begin{aligned} l^2 &= \frac{8\pi^2 m}{\hbar^2} \left(E_k + \frac{e^2}{4z_0} \right) \quad (l > 0), \\ k^2 &= \frac{-8\pi^2 m}{\hbar^2} E_k \quad (k > 0), \\ g^2 &= \frac{8\pi^2 m}{\hbar^2} \left(E_f + \frac{e^2}{4z_0} \right) \quad (g > 0), \\ f^2 &= \frac{8\pi^2 m}{\hbar^2} E_f \quad (f > 0), \end{aligned} \quad (6)$$

where the initial-state electron energy E_k is negative (bound electrons) and lies below the Fermi level, and the final-state energy $E_f = E_k + \hbar\omega$.

The coefficients a_k , b_k , and a_f , b_f in the above

wave-function expressions may be determined from continuity relations at $z = z_0$. The vector quantity \vec{a}_z in the above matrix element represents the z component of the vector potential associated with p -polarized-light excitation of the surface.

The above formalism of Mitchell-Makinson yields an expression for the current into vacuum resulting from the excitation of a single electron within the Fermi sea. The need to calculate the total absorbed energy due to surface excitation, and thus to evaluate the validity of the unperturbed-excitation-field assumption, prompted the calculation of the surface photocurrent excited back into the metal as well as the surface photocurrent into vacuum. To our knowledge, the only previous attempt to calculate total surface excitation in this manner is that of Wilems and Ritchie.²¹

The result of this extension of the Mitchell-Makinson formalism to the calculation of back excitation yields

$$(j_z)_{\text{back}} = (4\pi^2 em/\hbar g) |\langle M_g \rangle|^2, \quad (7)$$

in analogy with Eq. (1).

The expression for the matrix element for back excitation yields

$$\langle M_g \rangle = \frac{e/mc}{2\pi} \int_{-\infty}^{\infty} dz \left(\vec{a}_z \frac{\partial \psi_k}{\partial z} + \frac{1}{2} \psi_k \frac{\partial \vec{a}_z}{\partial z} \right) (\psi_f^+). \quad (8)$$

For back-excited electrons whose final-state wave functions have a z component of momentum sufficient for escape (excitation above threshold), the definitions for the wave functions ψ_k and ψ_f^+ are the same as in Eqs. (3)–(6). For final-state wave functions totally bound (back excitation below threshold), we have the modified definition

$$\begin{aligned} \psi_f^+ &= e^{-iG(z-z_0)} + a_f e^{iG(z-z_0)}, \quad z < z_0 \\ &= b_f W_{s/f, 1/2}(2fz), \quad z > z_0 \end{aligned} \quad (4a')$$

and $f^2 = -(8\pi^2 m/\hbar^2)E_f$ (E_f is negative for bound final states).

It is clear from the preceding expressions that the back excitation and surface photoemission in this formalism are completely determined by the fixed parameters of the electron density of the metal, escape barrier height, and by the detailed behavior of the normal component $\vec{a}_z(z)$ of the vector potential excitation field. The treatment of this field forms the essence of this paper's contribution to the calculation of the surface photoeffect.

We begin by noting that for ideally smooth surfaces, Maxwell's equations yield the ratio of \vec{a}_z just outside the surface z_0^+ to \vec{a}_z just inside the region of the surface-polarization charge z_0^- , as²²

$$\frac{\vec{a}_z(z_0^+, \phi, \omega)}{\vec{a}_z(z_0^-, \phi, \omega)} = \epsilon(\omega), \quad (9)$$

independent of the angle of incidence ϕ of the ex-

citation field. This charge region is typically around 1 Å thick. Schiff and Thomas²³ showed that if an exact quantum treatment of the detailed behavior of $\vec{a}_z(z)$ is attempted, the shape of $\vec{a}_z(z)$ is found to remain independent of angle of incidence within the region of the surface-polarization charge variation.²⁴

The implications of these conclusions are immediately clear. The angular variation in $\vec{a}_z(z, \phi)$ may be factored out of matrix elements for the excitation of each electron within the Fermi sea, leaving an expression which is a *characteristic* photoexcitation dependent only upon excitation energy, and a second factor, dependent only upon optical constants and angle of light incidence. This separation has the practical value of allowing one to carry out the rather tedious characteristic excitation calculation just once. This result may then be applied to a number of specific experimental situations by simply recalculating the appropriate angular factors.

Accordingly, we may begin by defining a normalized vector potential field in a nearly-free-electron metal as

$$\begin{aligned}\vec{s}_z(z, \omega) &\equiv \frac{\vec{a}_z(z, \phi, \omega)}{|\vec{a}_z(z_0^+, \phi, \omega)|}, \quad \omega \leq \omega_p/\sqrt{2} \\ &\equiv \frac{\vec{a}_z(z, \phi, \omega)}{|\vec{a}_z(z_0^-, \phi, \omega)|}, \quad \omega \geq \omega_p/\sqrt{2}\end{aligned}\quad (10)$$

where the rather synthetic redefinition of the normalized field for $\omega \geq \omega_p/\sqrt{2}$ is carried out in order to avoid the singularity which would otherwise occur in $\vec{s}_z(z)$ within the metal near the volume plasma frequency, $\omega = \omega_p$. Note that $\vec{s}_z(z)$ is continuous through $\omega_p/\sqrt{2}$, for a free-electron metal. If we now redefine matrix elements of Eqs. (2) and (8) in terms of $\vec{s}_z(z, \omega)$, and remove the angular factor to outside an integration over the appropriate initial states within the Fermi sphere,²⁵ we obtain an expression for the total photoexcitation current associated with some photon flux at an arbitrary angle of incidence. Dividing this current by $(\omega^2 \cos \phi / 2\pi c) |\vec{a}_i(\omega)|^2$, the incident photon flux per unit area (\vec{a}_i is the strength of the incident vector potential field), we obtain an expression for photoexcitation current per incident photon

$$J_I = \mathcal{F}_p(\phi) Y_{CH}(\omega), \quad (11)$$

where

$$\begin{aligned}\mathcal{F}_p(\phi) &\equiv \frac{1}{\cos \phi} \left| \frac{\vec{a}_z(z_0^+, \phi, \omega)}{\vec{a}_i(\omega)} \right|^2 \\ &= \frac{4 \cos \phi \sin^2 \phi |N|^2}{|N \cos \phi + \cos \phi''|^2}, \quad \omega \leq \omega_p/\sqrt{2} \\ &\equiv \frac{1}{\cos \phi} \left| \frac{\vec{a}_z(z_0^-, \phi, \omega)}{\vec{a}_i(\omega)} \right|^2\end{aligned}$$

$$\begin{aligned}&= \frac{1}{|N|^4 \cos \phi} \left| \frac{\vec{a}_z(z_0^+, \phi, \omega)}{\vec{a}_i(\omega)} \right|^2 \\ &= \frac{4 \cos \phi \sin^2 \phi}{|N|^2 |N \cos \phi + \cos \phi''|^2}, \quad \omega \geq \omega_p/\sqrt{2}\end{aligned}\quad (12)$$

for $N \equiv (\epsilon)^{1/2} = (\epsilon_1 - i\epsilon_2)^{1/2}$,²⁶ ϕ the angle of incidence, and ϕ'' the complex angle of refraction. The characteristic photoyield is of the form

$$Y_{CH}(\omega) = \left(\frac{e^3}{2\pi^2 m c \omega} \right) \int_{\text{limit}_\chi} d^3 k \left(\frac{|\langle \mathfrak{M}_\chi \rangle|^2}{\chi} \right), \quad (13)$$

where $\chi = f$ is forward emission and $\chi = g$ is back excitation. The redefined matrix elements are

$$\begin{aligned}\langle \mathfrak{M}_f \rangle &= \frac{(e/mc) b_f}{2\pi |b_f|^2} \\ &\times \int_{-\infty}^{\infty} dz \left(\vec{s}_z \frac{\partial \psi_k}{\partial z} + \frac{1}{2} \psi_k \frac{\partial \vec{s}_z}{\partial z} \right) [\psi_f^* - a_f^* \psi_f^*], \quad (14a)\end{aligned}$$

$$\langle \mathfrak{M}_g \rangle = \frac{e/mc}{2\pi} \int_{-\infty}^{\infty} dz \left(\vec{s}_z \frac{\partial \psi_k}{\partial z} + \frac{1}{2} \psi_k \frac{\partial \vec{s}_z}{\partial z} \right) (\psi_f^*). \quad (14b)$$

Specifying the limits of integration within the Fermi sphere, we obtain the final result:

$$Y(\omega)_{CH:\text{forward}} = \left(\frac{e^3}{2\pi m c \omega} \right) \int_{k_{\min}}^{k_F} dl (k_F^2 - l^2) \frac{|\langle \mathfrak{M}_f \rangle|^2}{f}, \quad (15a)$$

$$Y(\omega)_{CH:\text{back, above}} = \left(\frac{e^3}{2\pi m c \omega} \right) \int_{k_{\min}}^{k_F} dl (k_F^2 - l^2) \frac{|\langle \mathfrak{M}_g \rangle|^2}{g}, \quad (15b)$$

$$\begin{aligned}Y(\omega)_{CH:\text{back, below}} &= \left(\frac{e^3}{2\pi m c \omega} \right) \\ &\times \int_0^{k_{\min}} dl (k_F^2 - k_{\min}^2) \frac{|\langle \mathfrak{M}_g \rangle|^2}{g}, \quad (15c)\end{aligned}$$

where k_F is the Fermi vector, and $k_{\min}^2 = 0$ or $k_{\min}^2 = -(8\pi^2 m / h^2) (\hbar\omega + V_0)$, whichever is greater. $\langle \mathfrak{M}_f \rangle$ and $\langle \mathfrak{M}_g \rangle$ are defined in Eqs. (14) and ψ_f^* appropriate to Eqs. (15a) and (15b) is given by Eq. (4a), while ψ_f^* appropriate to Eq. (15c) is given by Eq. (4a'). Other relevant parameters are defined in Eqs. (3)–(6).

Physically, the characteristic photoyields defined in Eq. (15) are the yields that would occur per incident photon if the normal component of the field strength $\vec{a}_z(z)$ were somehow normalized so that its value just outside (inside) the surface was equal to the incident photon field strength for excitation energies less than (greater than) $\hbar\omega_p/\sqrt{2}$.

We have thus defined our emitted and back-excited surface photoexcitation in such a way that multiplying the characteristic yield by $\mathcal{F}_p(\phi)$ gives the surface excitation per incident photon for an arbitrary angle of incidence. The photoyield *per*

absorbed photon may be determined in a similar fashion by defining the field ratio

$$\mathcal{G}_p(\phi) \equiv \mathcal{F}_p(\phi) / \Delta R_p(\omega, \phi), \quad (16)$$

$$\Delta R_p \equiv 1 - R_p(\omega, \phi)$$

such that $\mathcal{G}_p(\phi)$ times the characteristic photoyield gives surface excitation per absorbed photon. The p subscripts refer to p -polarized light.

We may express $\mathcal{G}_p(\phi)$ in a more generally useful form by noting that for isotropic materials

$$\frac{4\pi\sigma/c}{\alpha(\phi) \cos\phi} \frac{|\vec{a}_z(z_0^+, \phi, \omega)|^2 + |\vec{a}_z(z_0^-, \phi, \omega)|^2}{|\vec{a}_i(\omega)|^2} = \Delta R_p(\phi), \quad (17)$$

where $\alpha(\phi)$ is the optical absorption coefficient for light excitation at angle ϕ , and $\sigma(\omega)$ is the optical conductivity of the medium. Thus

$$\begin{aligned} \mathcal{G}_p(\phi) &= \frac{\alpha(\phi)}{4\pi\sigma/c} \frac{|\vec{a}_z(z_0^+, \phi, \omega)|^2}{|\vec{a}_z(z_0^+, \phi, \omega)|^2 + |\vec{a}_x(z_0^+, \phi, \omega)|^2} \\ &= \frac{\text{Im}(N \cos\phi'') |N \sin\phi|^2}{N_r N_i (|\sin\phi''|^2 + |\cos\phi''|^2)}, \quad \omega \leq \omega_p / \sqrt{2} \\ &= \frac{\text{Im}(N \cos\phi'') |\sin\phi|^2}{|N|^2 N_r N_i (|\sin\phi''|^2 + |\cos\phi''|^2)}, \\ &\quad \omega \geq \omega_p / \sqrt{2}, \quad (18) \end{aligned}$$

where N_r and N_i refer to the real and imaginary parts of N . $\mathcal{G}_p(\phi)$ defined in this more general form is equally applicable for real or for complex angles of p -polarized-light incidence. In particular, if the complex angle $\phi_{sp}(\omega)$ representing the surface-wave (plasmon) mode of p -polarized light is used, then the resultant $\mathcal{G}_p(\phi_{sp})$ factor will yield surface photoexcitation per absorbed (decaying) surface wave, when multiplied by the characteristic surface photoyield.

At this point it is good to state explicitly that the ideal free-electron model is used to describe various physical phenomena throughout this paper whenever this model gives a good first-order approximation to the process of interest. More exact pictures are used only when the physical process of interest is forbidden within the free-electron model. Thus our analyses of surface excitation and surface-polarization charge-density variations are carried out based on the free-electron model, while the factor $\mathcal{G}_p(\phi)$ giving the surface excitation per absorbed photon (plasmon) necessarily includes the actual complex index of refraction N , reflective of the actual energy absorbed by the metal.

Proceeding with this view, the complex angle of incidence appropriate to a surface wave upon an ideally free-electron gas may be shown to be^{12,27}

$$\phi_{sp}(\omega) = \frac{1}{2}\pi - i\theta(\omega), \quad (19)$$

where

$$\theta(\omega) = \text{arccosh} |ck_{sp}(\omega)/\omega| \quad (20)$$

and

$$\omega^2 = \frac{1}{2}\omega_p^2 + c^2 k_{sp}^2 - (\frac{1}{4}\omega_p^4 + c^4 k_{sp}^4)^{1/2} \quad (21)$$

is the standard surface-wave dispersion relation for an ideal free-electron metal.

The results of this section have thus shown that surface-effect emission and back excitation may be factored into characteristic excitation terms independent of angle of exciting light incidence, and field ratio factors. The field factors $\mathcal{F}_p(\phi)$ and $\mathcal{G}_p(\phi)$, when multiplied by the characteristic excitation, give surface excitation per incident and per absorbed photon, respectively, for arbitrary angle of p -polarized-light incidence ϕ . The special case of surface-plasmon excitation is treated by assuming the complex angle of incidence of Eq. (19).

B. Surface-Polarization Charge

Perhaps the most significant contribution of the present calculation lies in the improved treatment of the normal component of the electromagnetic field in the vicinity of the surface. The derivation of the previous section presents a concise formalism for calculating the emitted and back-excited surface photoelectrons in terms of this component. While the normalized form of this field component is known in regions away from the surface-polarization charge,²²

$$\begin{aligned} \vec{s}_z(z_0^+, \omega) &= 1, & \omega \leq \omega_p / \sqrt{2} \\ &= \epsilon(\omega), & \omega \geq \omega_p / \sqrt{2} \\ \vec{s}_z(z_0^-, \omega) &= \epsilon(\omega)^{-1}, & \omega \leq \omega_p / \sqrt{2} \\ &= 1, & \omega \geq \omega_p / \sqrt{2} \end{aligned} \quad (22)$$

the variation in $\vec{s}_z(z, \omega)$ in the surface-polarization charge region between what is designated z_0^+ and z_0^- , is strongly dependent upon the dynamic screening behavior of the electron gas. Schiff and Thomas²³ first attempted a quantum solution of this problem, and Makinson⁴ extended their results, with further approximations, to a calculation of the surface photoeffect. Unfortunately, the essential features of the dynamic behavior of the electron gas was lost in the approximations of these treatments, but Makinson's work did serve to point out the importance of including the divergence term in the excitation Hamiltonian, and the sensitivity of the magnitude of the calculated surface effect to the details of surface-polarization charge variations.

While there has been no surface-effect calculation since that of Makinson which has attempted a treatment of surface-polarization charge variations, the great body of work concerned with dielectric response and charge-density fluctuations

in an electron gas provides a basis for the present treatment not available to Makinson. Some recent approaches to the problem of the dynamic behavior of an electron gas at a surface have been quite sophisticated,²⁸ but in the present treatment, we have chosen to take the most simple model capable of yielding the essential nature of the dependence of surface photoexcitation upon surface-polarization charge-screening effects. This model is the semiclassical Bloch hydrodynamic scheme as used by Crowell and Ritchie⁷ in the calculation of surface-wave fields and as applied by Melnyk and Harrison⁸ to the calculation of optical excitation fields near the surface.

The linearized form of the Bloch equations yields the dispersion relation

$$\Gamma^2 = [\omega_p^2 - \omega(\omega + i/\tau)]/\beta^2, \quad \beta^2 = \frac{3}{5} v_F^2 \quad (23)$$

(where $v_F = \hbar k_F/m$ is the Fermi velocity) for charge-density variations within the volume of an electron gas valid for $\omega > \omega_p$ (propagating waves) or $\omega < \omega_p$ (attenuating waves).²⁹ These equations assume an electron scattering rate τ^{-1} .³⁰ It was suggested by Sauter³¹ that similar charge-density waves should be generated at metallic surfaces by oblique-incidence p -polarized-light excitations. A more exact analysis by Melnyk and Harrison has shown that p -polarized-light induced charge-density waves propagating from the surface have the same dispersion relation [Eq. (23)] as volume charge-density waves. Predicted resonance effects for $\omega \geq \omega_p$ in these optically induced waves have been experimentally verified in thin films.^{32,33} Independently of this work, Ritchie *et al.*^{7,34} found that surface charge-density fluctuations associated with surface plasmons could also be determined from the Bloch equations. Spatial variations in these charge fluctuations for small-wave-number plasmons were in agreement with Eq. (23), consistent with the view of this paper that surface plasmons are a special case of p -polarized-light excitation. The above authors^{7,8} confirmed that at

distances from the surface greater than the surface-polarization charge thickness, the normalized field component $\vec{s}_z(z, \omega)$ remains as defined in Eq. (22) for both surface-plasmon and conventional p -polarized-light excitations. In the surface region, the field variation is defined by Eq. (23).

The simple picture discussed by Melnyk and Harrison⁸ and Crowell and Ritchie⁷ assumed a step discontinuity in the electron charge density at the surface. A more reasonable indication of the actual charge density at a metallic surface is given in Fig. 2 as calculated from the electron wave functions associated with an image charge surface potential. The charge variation is seen to occur over a distance comparable to the polarization charge region of appreciable variation in $\vec{s}_z(z, \omega)$ obtained from the Bloch equations.²⁹ Crude account of the variation in the unperturbed metallic charge density was taken in the present calculation by convolving the function $\vec{s}_z(z, \omega)$ with the derivative of the normalized charge density shown in Fig. 2. This operation served not only to affect an appropriate smearing of $\vec{s}_z(z, \omega)$, but also served to pin the exact location of the "surface" with respect to the wave functions involved in the calculation.

The above determination of the normal component of the vector potential field involved in surface photoexcitation is the first such treatment of the surface photoeffect to account for the dynamic or screening behavior of the electron gas. The treatment of $\vec{s}_z(z, \omega)$ avoids the field singularities at $\omega \approx \omega_p$ in previous treatments by Makinson⁴ and others, and enables us to carry out the present calculation to $\omega = \omega_p$ and beyond.

Numerical evaluations³⁵ of the characteristic surface excitations of Eq. (15) are plotted in Fig. 3 for a free-electron model having the parameters of Al (see Table I). The qualitative behavior of these curves indicates a very strong surface effect at energies below $\hbar\omega_p$, followed by the almost total suppression of the effect near the volume plasma energy.

The physical basis for this behavior may be appreciated by recognizing the surface effect as a photoexcitation process which occurs via momentum conservation through electronic reflection at the surface barrier, and through electronic interaction with the surface-polarization charge density. At excitation energies below the Al surface-barrier energy of 15.8 eV, some excited-state electrons will always lie near the threshold energy where momentum-conserving surface-barrier reflections are strong. At higher energies the strength of the surface effect diminishes as partial reflection of excited states decreases. Superimposed upon this effect is the electronic interaction with the surface-polarization charge as given by the

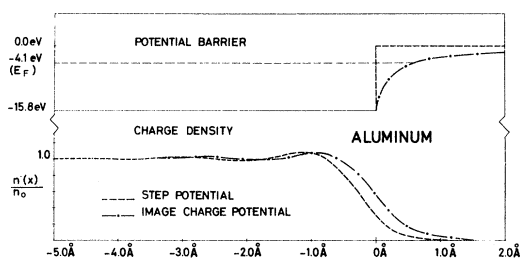


FIG. 2. Image charge surface potential (dot-dash curve), and stepped surface potential (dashed curve) for Al. Also shown are associated electron charge densities calculated from the electron wave functions forming the occupied-state solutions for these two potential barriers.

divergence term in the excitation Hamiltonian. At energies well below $\hbar\omega_p$, fields change rapidly near the surface, and the divergence term is large. Above the volume plasma energy, field discontinuities become small and the divergence term becomes negligible. The almost total suppression of the surface effect right at $\hbar\omega_p$ is associated with surface charge screening of the strong normal field component within the metal ($\vec{S}_z(z_0^-, \omega)/\vec{S}_z(z_0^+, \omega) = \epsilon(\omega)^{-1}$) to distances well away from the momentum-conserving surface region. This dynamic behavior of the surface-polarization charge is thus seen to have a fundamental influence on the strength of the surface photoelectric effect.

C. Calculation Sensitivity

Over the years, various surface-effect calculations have emphasized assumptions or approaches unique to their treatment to the neglect of problems of a more fundamental importance. The neglect of surface fields is a case in point. In this section we attempt to evaluate quantitatively the relative

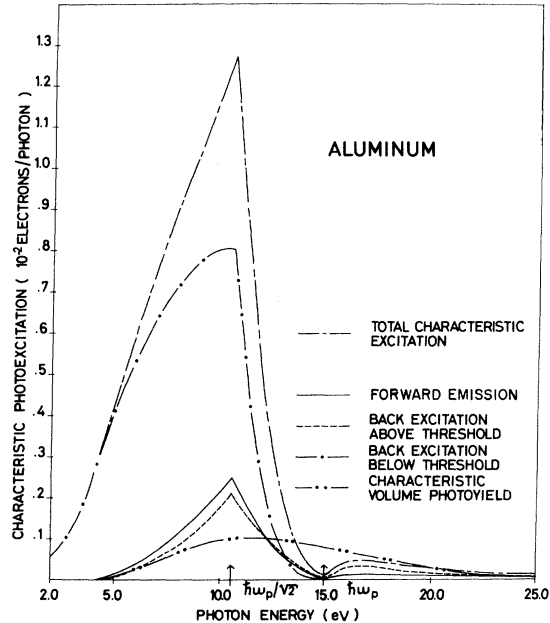


FIG. 3. Characteristic photoexcitation in the surface-effect theory and in the volume-effect theory. The solid curve is the forward or photoemitted component $Y_{\text{CH:forward}}$ of surface excitation. The dashed curve is the surface excitation back into the metal $Y_{\text{CH:back,above}}$ such that excited electrons have enough momentum normal to the surface to allow escape. The dot-dash curve represents surface back excitation for which excited electrons have insufficient momentum for escape, $Y_{\text{CH:back,below}}$. The long-short-dash curve represents the sum of the three contributions to total surface photoexcitation, $Y_{\text{CH:total}}$. Characteristic photoexcitation in the isotropic excitation volume-effect theory, $Y_{\text{CH:volume}}$ is shown as a dot-dot-dash curve.

TABLE I. Aluminum optical constants and other parameters used in the present calculation.

Aluminum							
eV	$-\epsilon_1^a$	ϵ_2^a	eV	$-\epsilon_1^b$	ϵ_2^b	Parameter	eV
2.0	44.2	15.25	6.5	4.40	0.418	$\hbar\omega_p$	14.9 ^c
2.5	29.6	7.21	7.0	3.63	0.325		
3.0	20.7	3.89	7.5	3.00	0.260	E_F	11.7 ^d
3.5	14.9	2.33	8.0	2.47	0.207	$= \hbar^2 k_F^2 / 2m$	
4.0	11.4	1.56	8.5	2.07	0.173		
4.5	9.2	1.15	9.0	1.75	0.147	V_0	15.8 ^e
5.0	7.75	0.91	>9.0			Drude model ^c	
5.5	6.40	0.70				$\epsilon_1 - i\epsilon_2^f$	2.05 ^g
6.0	5.30	0.54				$\equiv 1 - \omega_p^2 / \omega(\omega - i/\tau)$	

^aThe optical constants, 2.0–6.0 eV, were matched to the reflectance values of Ref. 36.

^bThe optical constants, 6.5–9.0 eV, were matched to the reflectance values of Refs. 30 and 37.

^cThe optical constants above 9.0 eV were taken from the Drude-model match to experimental reflectance in Ref. 30. The appropriate Drude parameters are also defined in that paper.

^dThe calculation of E_F was based on a free-electron model and the known valence-electron density of Al.

^e V_0 was determined from E_F and the measured 4.1-eV Al work function of Ref. 38.

^fThe sign of $i\epsilon_2$ has been changed in accordance with Ref. 26.

importance of various assumptions and parameters used in the present calculation.

It is a unique aspect of this calculation that the interaction between the surface-polarization charge density and surface excited electrons has been included. An important result of that approach is emphasized in Fig. 4, which shows an enormous peak in the back-excited surface excitation for energies just above $\hbar\omega_p$. No such peak appears in the calculated forward emission. The peak is clearly associated with the decay of optically excited volume plasmons into single-electron excitations as the plasmons propagate from the surface into the metal. The unreasonable magnitude of the peak points out a fundamental shortcoming of the present perturbative calculation. While the effect of the polarization charge density upon the induced surface excitation has been included, there has been no attempt to self-consistently include the effect of exciting electrons back on the assumed charge density. This problem is clear with regard to the failure of Eq. (23) to include a strong single-particle decay-damping term once the frequency for such processes has been attained, but a similar breakdown in the semiclassical Bloch formalism leading to Eq. (23) must occur at all frequencies. Ideally, the possibility of momentum-conserving excitations of electrons at the surface must be included self-consistently in any treatment of the dynamic behavior of an electron gas near a surface.

The curves designated Γ_{damped} in Fig. 4 were calculated by arbitrarily replacing $\Gamma \equiv \Gamma_r + i\Gamma_i$ of

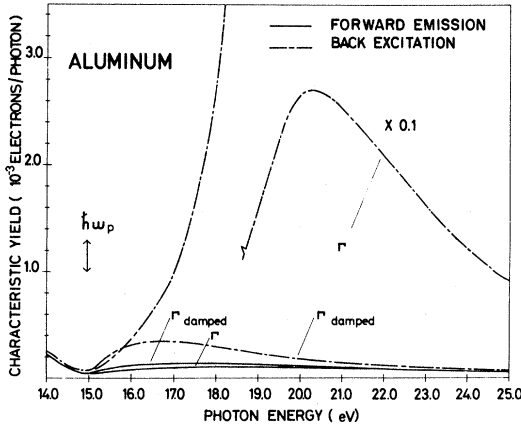


FIG. 4. "Plasmon-quasiparticle decay" inherent in the present surface-effect calculation is indicated by the enormous peak in back-excited electrons, $Y_{\text{CH};\text{back,above}}$ (dot-dash curve) for energies just above $\hbar\omega_p$. Failure to conserve momentum prevents a similar peak for emitted electrons (solid curve). The curves designated Γ_{damped} represent a crude attempt to account for damping of the surface-polarization charge-density waves in the surface-effect calculation.

Eq. (23) with $\Gamma_{\text{damped}} \equiv \Gamma_i + i\Gamma_i$ in the expressions for the surface photoeffect. The substitution had negligible effect on the forward emission, and the calculated curves in Fig. 3 for $\omega > \omega_p$ are based on this substitution.

We have stated qualitatively that the surface-polarization charge-density effects the surface photoeffect in essentially two ways. It couples strongly to individual electrons via the divergence term in the excitation Hamiltonian, and it screens the excitation fields away from the surface at frequencies near ω_p . These two effects are distinctly and explicitly shown in Fig. 5. The characteristic forward emission is calculated over a range of frequencies for a normal component $\vec{s}_z(z, \omega) \equiv \vec{s}_z(z, 10.5 \text{ eV})$, for $\vec{s}_z(z, \omega) \equiv 1.0$, and for the correct value $\vec{s}_z(z, \omega)$. The field, $\vec{s}_z \equiv 1.0$, constant in space and frequency, clearly yields no contribution to the divergence term and results in a calculated forward emission which is considerably less than the emission resulting from the inclusion of divergence term effects in the 10.5-eV field calculation. The divergence-free field calculation is necessarily less than the correct field calculation at energies below $\hbar\omega_p$, but the correct field treatment actually dips below the constant field calculation for ω near and above ω_p , as the fields in the correct treatment are screened away from the surface region. The surface charge and surface screening subsides at energies well above ω_p , and the correct field calculation approaches the divergence-free calculation.

There are three additional checks on the calcu-

lation sensitivity which deserve mention. All were carried out in the low-energy region ($\omega \leq \omega_p/\sqrt{2}$). The first was a comparison of the calculation of the the forward emission calculated assuming a step rather than image surface potential (Fig. 2). The modified calculation was 10% lower at 10.5 eV, 30% lower at 6.0 eV, and a negligible fraction of the image charge calculation at threshold. The second check was to translate the excitation field $\vec{s}_z(z, \omega)$. The resultant calculated forward emission was found to change by $- (+) 5\%$ over the entire range $\omega < \omega_p/\sqrt{2}$ for a shift of $+ (-) 0.1 \text{ \AA}$. In the third and final check, the polarization-charge decay coefficient Γ was increased by 50% and decreased by 33%. The resultant change in the calculated forward emission was $\sim \pm 20\%$ near $\hbar\omega_p/\sqrt{2}$, diminishing to well under $\pm 5\%$ near threshold.

III. DISCUSSION

The preceding calculation has been structured in such a way that the characteristic photoexcitation curves of Fig. 3 may be easily adapted to the calculation of surface photoexcitation in specific physical situations simply by multiplying by the appropriate field ratio factors such as $\mathcal{F}_p(\phi)$ or $\mathcal{G}_p(\phi)$. The evaluation of these and other factors for Al are based on the optical constants and other parameters of Table I.^{30,36-38}

A. Possible Optical Effects

It has been emphasized that this is a perturbative calculation which makes no attempt to account for the effect of surface excited electrons back onto the assumed variation of the optical (plasmon) excitation fields or surface-polarization charge. One point where the perturbative assumption can definitely be said to break down, is when the calculated surface ex-

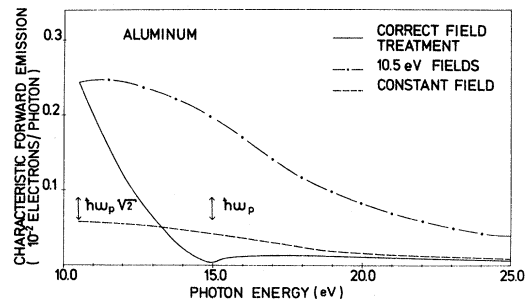


FIG. 5. Characteristic forward emission $Y_{\text{CH};\text{forward}}$ assuming various forms for the normal component $\vec{s}_z(z, \omega)$ of the excitation field. The dot-dash curve assumes $\vec{s}_z(z, \omega) \equiv \vec{s}_z(z, 10.5 \text{ eV})$. The dashed curve assumes $\vec{s}_z(z, \omega) \equiv 1.0$, and the solid curve assumes the correct form for $\vec{s}_z(z, \omega)$. Note that the surface-charge-induced variations in $\vec{s}_z(z, \omega)$ in space and frequency cause an enhancement in the surface effect at low energies and a suppression near $\hbar\omega_p$.

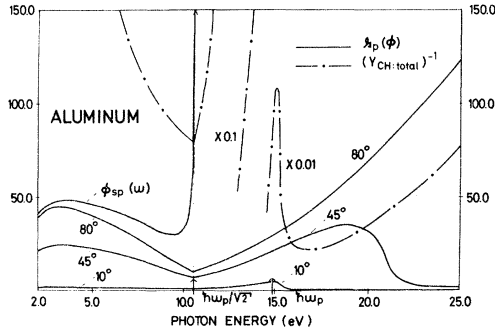


FIG. 6. Plots of the field ratio factor $\mathcal{G}_p(\phi)$ vs angle of light incidence (solid curves). The value of this factor increases with angle and is particularly large for the complex angles $\phi_{sp}(\omega)$ characteristic of surface waves. When $\mathcal{G}_p(\phi)$ exceeds $(Y_{CH:total})^{-1}$ (dot-dash curve), the surface effect can be said to dominate the energy loss per absorbed photon or per decaying surface wave (plasmon).

citation approaches or exceeds one electron per *absorbed* photon (decaying plasmon). Of comparable interest is the fact that when and if this criteria is met, surface excitation will come to dominate the total energy absorbed by the metal and thus should be directly observable in optical as well as in photoemission experiments.

In Fig. 6 we see plots of $\mathcal{G}_p(\phi)$ for various real angles of light incidence and for $\phi = \phi_{sp}(\omega)$. The $Y_{CH:total}$ indicated in the figure is the total characteristic surface excitation plotted in Fig. 3. Clearly, the definition of \mathcal{G}_p implies that the total surface excitation per absorbed photon will exceed one electron whenever $\mathcal{G}_p(\phi)$ exceeds $(Y_{CH:total})^{-1}$. Thus $(Y_{CH:total})^{-1}$ has also been plotted on Fig. 6 in order to establish very quickly under what circumstances surface optical effects or the breakdown of our perturbative calculation might occur. One sees immediately that $\mathcal{G}_p(\phi)$ remains appreciably less than $Y_{CH:total}^{-1}$ for all real angles of light incidence. It is only when $\mathcal{G}_p(\phi)$ is calculated for the complex angles of incidence characteristic of surface waves that $\mathcal{G}_p(\phi)$ exceeds $Y_{CH:total}^{-1}$, and by an appreciable amount. This is a first example of a general conclusion of this paper: *Surface waves (plasmons) form a uniquely effective mode of p-polarized-light excitation of the surface photoelectric effect.* The physical origin of this effect is the strong concentration of high- k plasmon energy near the surface.

The strength of the total surface excitation per decaying plasmon is perhaps better indicated in the plot of $\mathcal{G}_p(\phi_{sp})Y_{CH:total}$ vs plasmon wave vector in Fig. 7. In an attempt to take crude account of the breakdown of our perturbative calculation, we have redefined the total excitation:

$$(\mathcal{G}_p Y_{CH:total})' \equiv 1 - \exp(-\mathcal{G}_p Y_{CH:total}). \quad (24)$$

In either plot, however, one sees that surface excitation comes to dominate the plasmon-decay process for surprisingly small plasmon wave vectors.

As a final comment on the question of possible surface optical effects, one notes that $\mathcal{G}_p(\phi)$ diverges to infinity in real metals as $\omega \rightarrow 0$ and $\%R_p$ goes to 1.0. [The apparent dropoff in $\mathcal{G}_p(\phi)$ near 2.0 eV in Al, Fig. 6, is related to the interband transitions occurring in Al near 1.4 eV.] This is equivalent to saying that volume photoexcitation becomes quite small at low energies. Total surface excitation $Y_{CH:total}$ was calculated in the limit $\omega \rightarrow 0$, but it was found that it decreased more rapidly than $\mathcal{G}_p(\phi, \omega)$ increased. The ratio of surface to volume absorbed energy for oblique angles of incidence was found to approach zero as $\omega \rightarrow 0$.

B. Volume- and Surface-Effect Photoemission

In the previous section we dealt with the question of whether the surface effect could dominate the total absorbed energy and found that our calculation implied such effects were only appreciable in plasmon excitation. A question that has been of much greater historical interest is the question of the relative strengths of the surface-vs-volume photoeffects in photoemission under various experimental circumstances. The problem of obtaining a general answer to this question on the basis of our surface-effect calculation is complicated by the problem of selecting a proper model for the volume photoeffect. Mahan¹⁹ has recently pointed out that severe directionality effects occur with volume-effect photoexcitation in the monovalent alkali metals. Such sharp directionality should be subdued in trivalent Al, and it may be reasonably accurate to assume isotropic excitation, and a rela-

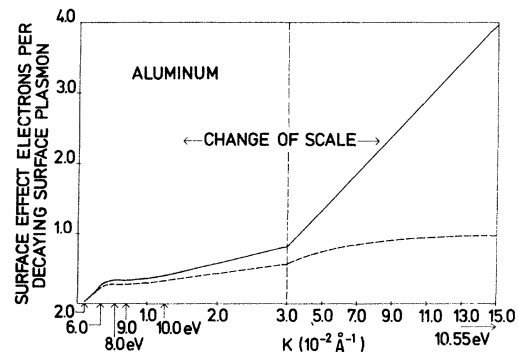


FIG. 7. Total surface photoexcited electrons $\mathcal{G}_p(\phi_{sp})Y_{CH:total}$ per decaying surface plasmon (solid curve). The curve is vs plasmon wave vector, but plasmon energy is also indicated. The modified expression, $1 - \exp(-\mathcal{G}_p Y_{CH:total})$ (dashed curve) is also shown. Note when these curves approach 1.0, surface excitation comes to dominate plasmon decay.

tively simple volume-effect model.

It will be assumed in the discussion that follows that Al electron energy levels are unperturbed from free-electron values, and that volume-effect excitation of these electrons is isotropic and occurs with equal probability for all accessible electrons within the Fermi sea. A rather simple isotropic excitation volume-effect model then follows. The normalized distribution in electron energy E , of photoexcited electrons becomes

$$D(E, \hbar\omega) = \gamma_0(E - \hbar\omega - V_0)^{1/2},$$

$$\hbar\omega + V_0 < E < \hbar\omega + V_0 + E_F, \quad \hbar\omega > E_F \quad (25)$$

$$E_F < E < \hbar\omega + V_0 + E_F, \quad \hbar\omega < E_F,$$

where γ_0 is the normalization constant. If one assumes that all excited electrons can reach the surface and that the surface escape probability is given by a classical escape cone, then the photoyield that one expects per absorbed photon is given by

$$y(\hbar\omega) = \int S(E)D(E, \hbar\omega) dE,$$

$$S(E) = 1 - [1/(1 - E/V_0)]^{1/2}. \quad (26)$$

Of course, only half of the excited electrons move towards the surface, and many of those are scattered. The number reaching the surface may be accounted for by the factor $\frac{1}{2}\alpha(\phi, \hbar\omega)l_e(\hbar\omega)$, where $\alpha(\phi, \hbar\omega)$, the optical-absorption coefficient, is the reciprocal of the optical energy penetration depth and $l_e(\hbar\omega)$ is an effective escape depth of the primary (unscattered) electrons. Incorporating this factor and recalling the identity (17), we obtain the volume effect photoyield per incident photon:

$$Y_{\text{volume}}(\hbar\omega) = \left(\frac{|\vec{a}_z(z_0^+, \phi, \omega)|^2 + |\vec{a}_x(z_0^+, \phi, \omega)|^2}{|\vec{a}_i(\omega)|^2 \cos\phi} \right) \times \left(\frac{(4\pi\sigma/c)l_e(\hbar\omega)y(\hbar\omega)}{2} \right). \quad (27)$$

We digress at this point to recall that the surface photoeffect in Eq. (15) was defined as a characteristic photoyield, independent of the angle of incidence of the exciting optical (plasmon) fields. It will prove extremely useful to define the volume photoyield in a similar fashion. The physical definition of the characteristic surface-effect photoemission of Eq. (15) was the photoyield per normally incident photon which would occur if the field strength $\vec{a}_z(z, \omega)$ could somehow be normalized so that its value just outside the surface was equal to the incident photon field strength, over the region of the surface illuminated by this photon. If we define a characteristic volume photoyield from Eq. (27)

$$Y_{\text{CH:volume}}(\hbar\omega) \equiv \frac{(4\pi\sigma/c)l_e(\hbar\omega)y(\hbar\omega)}{2} \quad (28)$$

one sees that this characteristic volume photoyield is the yield per normally incident photon which would occur if the total field strength inside the metal could somehow be normalized so that its value just inside the surface was equal to the incident field strength, over the region of the surface illuminated by this photon. With these physically consistent definitions, the ratio of forward surface effect emission to volume effect emission for an arbitrary angle of excitation is given simply by

$$S/V = \mathcal{V}_p(\phi) Y_{\text{ratio}}(\hbar\omega),$$

$$Y_{\text{ratio}}(\hbar\omega) \equiv \frac{Y_{\text{CH:forward}}(\hbar\omega)}{Y_{\text{CH:volume}}(\hbar\omega)}, \quad (29)$$

where all angular effects are contained in the field ratio

$$\mathcal{V}_p(\phi) \equiv \frac{\mathcal{F}_p(\phi) |\vec{a}_i(\omega)|^2 \cos\phi}{|\vec{a}_z(z_0^-, \phi, \omega)|^2 + |\vec{a}_x(z_0^-, \phi, \omega)|^2}$$

$$= \frac{|\vec{a}_z(z_0^+, \phi, \omega)|^2}{|\vec{a}_z(z_0^-, \phi, \omega)|^2 + |\vec{a}_x(z_0^-, \phi, \omega)|^2}$$

$$= \frac{|N \sin\phi|^2}{|\sin\phi''|^2 + |\cos\phi''|^2}, \quad \omega \leq \omega_p/\sqrt{2},$$

$$= \frac{|\vec{a}_z(z_0^+, \phi, \omega)|^2}{|\vec{a}_z(z_0^-, \phi, \omega)|^2 + |\vec{a}_x(z_0^-, \phi, \omega)|^2}$$

$$= \frac{|\sin\phi|^2}{|N|^2 (|\sin\phi''|^2 + |\cos\phi''|^2)}, \quad \omega \geq \omega_p/\sqrt{2}. \quad (30)$$

A comparison of the relative strengths of the surface and volume photoeffects thus reduces to an evaluation of $Y_{\text{ratio}}(\hbar\omega)$ and an evaluation of $\mathcal{V}_p(\phi, \omega)$ for specific experimental situations.

$Y_{\text{CH:volume}}(\hbar\omega)$ has $l_e(\hbar\omega)$ as its only free parameter. This was determined for Al between 6.0 and 11.5 eV by analysis of experimental smooth-surface photoyield data on Al.¹¹ Below 6.0 eV, values for $l_e(\hbar\omega)$ were set equal to $l_e(6.0 \text{ eV})$, while above 11.5 eV, values of $l_e(\hbar\omega)$ were linearly tapered from the $l_e(\hbar\omega)$ values at 11.5 eV to its value determined by Geselle and Arakawa at 22 eV.³⁹ The resultant evaluation of $Y_{\text{CH:volume}}(\hbar\omega)$ of Eq. (28) is plotted in Fig. 3, while the reciprocal of Y_{ratio} is shown in Fig. 8.

A quick glance at the plots of $\mathcal{V}_p(\phi, \omega)$ and $(Y_{\text{ratio}})^{-1}$ of Fig. 8 indicate the total dominance of the surface effect over the volume effect at energies near threshold and oblique angles of incidence, followed by the almost complete suppression of the surface-to-volume ratio near $\hbar\omega_p$. This suppression near the plasma energy is a result of surface charge screening effects as previously discussed, and shows itself as a sharp null in Y_{ratio} near $\hbar\omega_p$. Of greater significance are the large ratios of surface-to-volume excitation which occur at low energies. This enhancement at low ω is clearly an op-

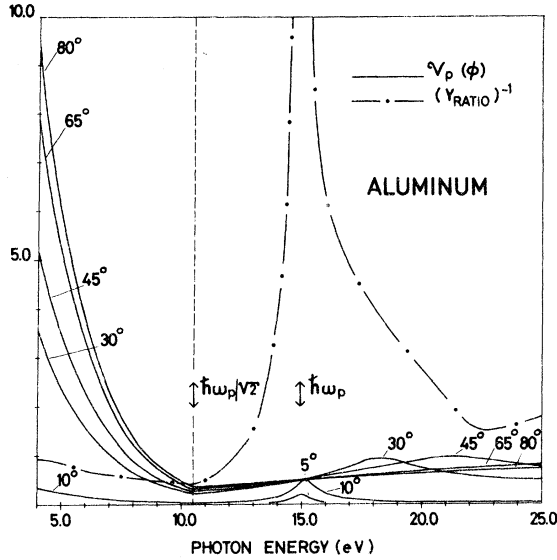


FIG. 8. Plots of the field ratio factor $\mathcal{U}_p(\phi)$ vs angle of light incidence (solid curves). Note the enormous enhancement in this factor at low energies and high angles of incidence. The surface effect dominates isotropic volume effect photoemission whenever \mathcal{U}_p exceeds $(Y_{\text{ratio}})^{-1}$ (dot-dash curve).

tical effect, totally associated with the large values of the field ratios $\mathcal{U}_p(\phi, \omega)$. Noting the definition of \mathcal{U}_p in Eq. (30), we see that the large values of \mathcal{U}_p at low energies may be directly interpretable as resulting from the exclusion of the macroscopic fields from the volume of the metal. Summarizing these results, our calculations indicate volume-effect photoemission remains comparable to or greater than surface emission for oblique angles of incidence at most excitation energies. It is only at low excitation energies, where the macroscopic excitation fields are excluded from the volume of the metal, that surface-effect photoemission can grow to many times the volume photoemission.

C. Possible Experimental Implications

There remains the question of how to experimentally observe the surface photoelectric effect, whether it be in the surface wave (plasmon) or direct optical mode of excitation. The strong plasmon mode of surface-effect excitation can only occur through the intermediary of surface roughness and the experimental details of roughness-aided optical excitation and decay of these surface waves have been extensively described in the literature^{11,37,40} and will not be reviewed in this section. Rather we concentrate on a discussion of the possibilities of experimentally observing the somewhat weaker, but historically more important, optical mode of surface excitation. This mode of excitation occurs without the intermediary of surface

roughness, and in fact the presence of such roughness serves only to obscure a simple experimental observation of the surface effect, a point of historical interest.³ It was implied in the discussion of Fig. 1, and is assumed in the discussion of this section, that it is experimentally possible to produce films of certain nearly-free-electron metals which are sufficiently smooth so that roughness-aided surface-wave excitation can be ignored except in the immediate vicinity of the surface plasma energy. It may also be assumed that the obscuring effects of roughness in optical excitation can be ignored at all frequencies.

When such specular surfaces are obtained, the detection of the surface effect in optical excitation can be simply achieved through the measurement of the "vector ratio"⁴¹

$$\frac{Y_p(\hbar\omega, \phi)}{Y_s(\hbar\omega, \phi)} = \frac{Y_{p,\text{volume}}(\hbar\omega, \phi) + Y_{p,\text{surface}}(\hbar\omega, \phi)}{Y_{s,\text{volume}}(\hbar\omega, \phi)}, \quad (31)$$

where Y_p and Y_s refer to the experimentally observed photoyields for p and for s polarized light excitation. Equation (31) assumes only that the surface and volume photoeffects may be considered additive.^{6,19} Clearly, (31) reduces to

$$\frac{Y_p(\hbar\omega, \phi)}{Y_s(\hbar\omega, \phi)} = \frac{Y_{p,\text{volume}}(\hbar\omega, \phi)}{Y_{s,\text{volume}}(\hbar\omega, \phi)} [1 + \mathcal{U}_p(\phi) Y_{\text{ratio}}(\hbar\omega)] \quad (32)$$

if we recall our definition of $\mathcal{U}_p Y_{\text{ratio}}$ as the ratio of surface-to-volume effect photoemission for p -polarized light. The virtue of the approach of measuring the vector ratio lies in the fact that while photoyield in the volume theory depends strongly upon the optical-absorption coefficient α , the electron escape depth l_e , reflectance,⁴² and the polarization of the exciting light,¹⁹ the vector ratio of yields within the volume theory at energies that we will find of interest⁴³ depends strongly only upon the reflectance ratio $[1 - R_p(\hbar\omega, \phi)] / [1 - R_s(\hbar\omega, \phi)] \equiv \Delta R_p / \Delta R_s$. The ratio $\Delta R_p / \Delta R_s$, and thus $Y_{p,\text{volume}} / Y_{s,\text{volume}}$, may be reliably determined in terms of well-known optical constants of the metal. Any percent deviations in the experimental Y_p / Y_s from $Y_{p,\text{volume}} / Y_{s,\text{volume}}$ may then be unambiguously attributed to the factor $\mathcal{U}_p Y_{\text{ratio}}$,⁴⁴ provided only that $\mathcal{U}_p Y_{\text{ratio}}$ is sufficiently large to exceed the small uncertainties in the calculated $Y_{p,\text{volume}} / Y_{s,\text{volume}}$.

A summary of the experimental circumstances under which the ratio $\mathcal{U}_p Y_{\text{ratio}}$ might be expected to be both appreciable and measurable is provided in Fig. 9. The solid curve $\mathcal{U}_p(80^\circ) Y_{\text{ratio}}$ in Fig. 9 is probably the single most important result in the calculations of this paper. It indicates that the surface-to-volume ratio at grazing incidence and near threshold becomes so large as to introduce

an increase in the total vector ratio of almost 1000% over what one would expect in a simple volume-effect theory. Note that the plots of $\mathcal{V}_p(\phi)$ in Fig. 8 are monotonically increasing in ϕ for $\omega < \omega_p$, and somewhat insensitive to ϕ for $\omega > \omega_p$. Thus $\mathcal{V}_p Y_{\text{ratio}}$ at grazing incidence is about as large as one could expect to observe. The relatively small value of $\mathcal{V}_p(80^\circ) Y_{\text{ratio}}$ near and above ω_p is also significant, both as it relates to the difficulty in observing the surface effect at these energies, and as it relates to possible obscuring effects of surface excitation in oblique light incidence photoyield measurements such as those recently reported on by Geselle and Arakawa.³⁹

A large magnitude for the ratio $\mathcal{V}_p Y_{\text{ratio}}$ does not necessarily imply an easily observed effect. The absolute magnitude of the surface-effect photocurrent must also be appreciable, and thus the surface effect yield per incident photon at grazing incidence, $\mathcal{F}_p(80^\circ) Y_{\text{CH:forward}}(\hbar\omega)$ has been plotted in Fig. 9. Figure 10 allows one to see the variation in this photocurrent with angle of incidence. We note that at low energies, peaks in the photocurrent occur at high angles of incidence while at higher energies, peaks occur at lower angles.

One can make the very specific conclusion on

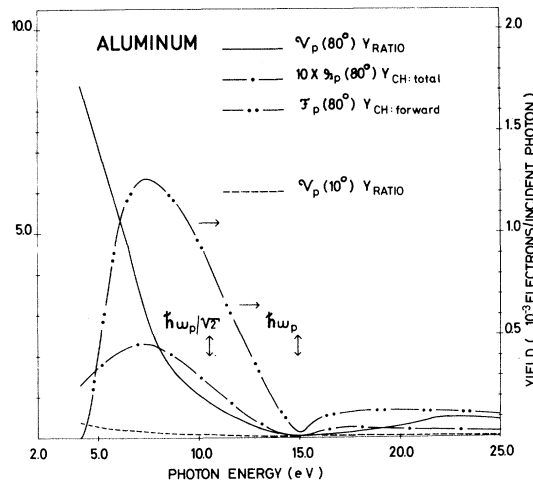


FIG. 9. Summary graph for optical excitation of the surface effect. The solid curve $\mathcal{V}_p(80^\circ) Y_{\text{ratio}}$ shows the ratio of surface-effect to volume-effect photoemission for excitation at 80° angle of incidence. Note the surface effect exceeds the volume effect at low energies by almost a factor of 10. The absolute magnitude of the surface-effect yield at 80° $\mathcal{F}_p(80^\circ) Y_{\text{CH:forward}}$ is also shown (dash-dot-dot curve), as is an expanded plot of the fractional total energy absorbed by the surface effect, $10 \times \mathcal{G}_p(80^\circ) Y_{\text{CH:total}}$ (dot-dash curve). A special plot of the ratio of surface-to-volume photoemission $\mathcal{V}_p(10^\circ) Y_{\text{ratio}}$ is shown for 10° , thought to be comparable to the surface angle presented to normally incident light by typical real smooth surfaces. Note the surface effect is negligible except at lowest energies.

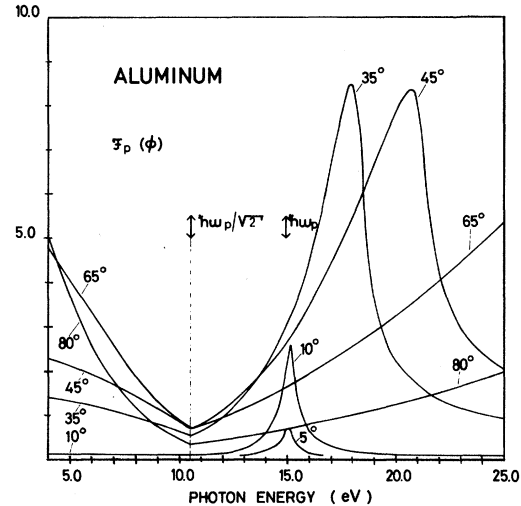


FIG. 10. Plots of the field ratio factor $\mathcal{F}_p(\phi)$ vs angle of light incidence. Note that the magnitude of this factor peaks at high angles for low energies, and peaks at low angles for high energies.

the basis of curves in Figs. 9 and 10 that the optically induced surface effect may be most easily and unambiguously determined in Al by measuring the vector ratio of photoyield in Al at high angles of incidence and at energies 1–2 eV above the photoemissive threshold.

As a final point, we note that the fractional energy absorbed $[\mathcal{G}_p Y_{\text{CH:total}}(\hbar\omega)]$ in electrons per absorbed photon] by the surface effect is also plotted for grazing incidence (80°) in Fig. 9 and indicates, as already discussed, that this quantity is always quite small for all possible energies of excitation. The ratio of surface-to-volume photoemission $\mathcal{V}_p Y_{\text{ratio}}$ is also shown plotted for 10° in Fig. 9. This angle is thought to be comparable to the effective angle presented to normally incident light by the smoothest metallic surfaces typically prepared in actual experiments.¹¹ The very low value of this ratio serves as a justification for our ignoring the importance of roughness in discussing direct optical excitation of the surface effect. It also tends to confirm that normal incidence photoexcitation of smooth surfaces should be regarded as a volume effect in all but the most nearly-free-electron metals, and even in these the surface effect should be considered significant only at lowest energies.

IV. COMPARISON WITH EXPERIMENT

Two questions naturally arise in comparing the implications of our calculations with experiments: Is there any existing experimental evidence for the surface photoelectric effect and, a related question of historical importance, why have so many previous attempts to detect experimentally the sur-

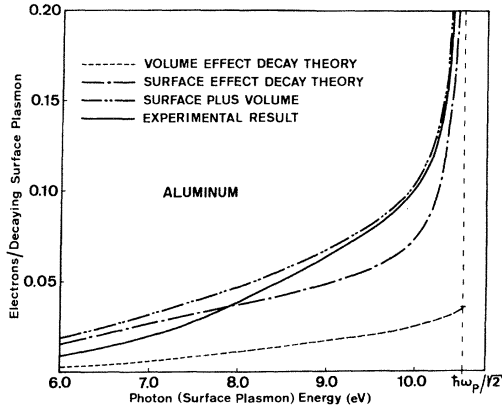


FIG. 11. Photoemitted electrons per decaying surface plasmon. Experimental results are given by the solid curve (Ref. 11). The isotropic volume-effect calculation $[(\mathcal{G}_p(\phi_{sp})/\nu_p(\phi_{sp})) Y_{CH:volume}(\hbar\omega)]$ is given by the dashed curve, and the dot-dash curve represents the surface-effect calculation $\mathcal{G}_p(\phi_{sp}) Y_{CH:forward}(\hbar\omega)$. The dot-dot-dash curve is the sum of volume- and surface-effect theories.

face effect failed? These two questions conveniently divide into a consideration of the surface wave (plasmon) vs the optical mode of p -polarized light excitation of the surface effect.

Our calculations imply that the *plasmon mode* of excitation should result in the strongest surface photoeffect, and in fact recent plasmon-decay data provide the only strong evidence to date for the surface effect.¹¹ An extensive discussion of the experimental approach to detecting this effect is found in Ref. 11, so this topic was neglected in Sec. III C. Nevertheless it is useful to review and expand upon the results of Ref. 11 in this section in view of the improved calculations of the present paper.

A possible method of detecting *optical* excitation of the surface effect was described in Sec. III C, and it is suggested in the present section that the historical failure to observe the surface effect in the alkali metals through such methods may be due to peculiarities in the monovalent alkali metals that make them ill-suited to such an approach.

A. Experimental Evidence in Surface-Wave Decay

1. Photoyield per Decaying Surface Plasmon

A preliminary report of a comparison of the experimental results of Ref. 11 for Al with the surface-wave decay calculations of the present paper for Al has already been given,¹³ but will be reviewed. The experimental yield per decaying surface wave was determined by measuring both the induced reflectance drop and photoyield increase associated with coupling to surface waves.¹¹ This result is shown plotted vs plasmon energy in Fig.

11. Also shown are the calculated photoyields in both the volume- and surface-effect theories.

The volume-effect curve per decaying plasmon is calculated from the same isotropic excitation model described in Sec. III.⁴⁵ It is given by

$$Y_{\text{volume/absorbed photon}}(\hbar\omega) = [\mathcal{G}_p(\phi_{sp})/\nu_p(\phi_{sp})] Y_{CH:volume}(\hbar\omega), \quad (33)$$

as implied in Eqs. (16) and (29). The surface-effect calculation is simply $\mathcal{G}_p(\phi_{sp}) Y_{CH:forward}(\hbar\omega)$ [$\mathcal{G}_p(\phi_{sp}) Y_{CH:total}(\hbar\omega)$ was plotted for surface waves in Fig. 7].

Clearly, the sum of surface- and volume-effect calculations give excellent agreement with the experimental yield data at high plasmon energies, an agreement which the isotropic volume effect is totally unable to achieve. These high- k surface-wave decay data provide what are at the very least unquestionable evidence for the breakdown of isotropic volume-effect theory, but which are more realistically viewed as the most simple and concise evidence available for the surface effect. The raw experimental data¹¹ indicated plasmon-induced yield increases of from 0.15 to 0.25 electrons per additionally absorbed photon near 10.5 eV, depending upon the surface studied. In the isotropic volume-effect theory the escape cone is so narrow at these energies that less than 0.04 electrons can escape per decaying plasmon, even if we assume an infinite inelastic scattering length l_e . Significantly the pure surface effect at these energies would give about 0.20 emitted electrons per decaying plasmon or absorbed photon (note the ratio of $Y_{CH:forward}/Y_{CH:total}$ at 10.5 eV in Fig. 3). It should be mentioned that if we had attempted to compensate for the perturbative nature of our calculation, as was done in Fig. 7, then the agreement between experiment and theory at these high energies would not be quite as good.

At lower energies, the plasmon-decay yield continues to be much stronger than the volume theory would indicate, and while the surface theory is significantly higher than experiment, it does provide a good explanation for the strong experimental result. The sensitivity of the surface calculation to several parameters discussed in Sec. II makes the experimental disagreement with the surface theory much more easily justified than the disagreement with the volume theory.

Although the calculation of this paper is carried out for Al, the implications of these results should be applicable to all nearly-free-electron metals. There have been no quantitative measures of the strength of the photoyield from surface waves in metals other than Al, but recent electron distribution curves (EDC's) taken on other metals provide good qualitative confirmation of the surface effect

in plasmon decay. Implications of our calculations and experiments discussed are that plasmon decay provides a uniquely effective means of exciting the surface effect, even on relatively smooth surfaces.

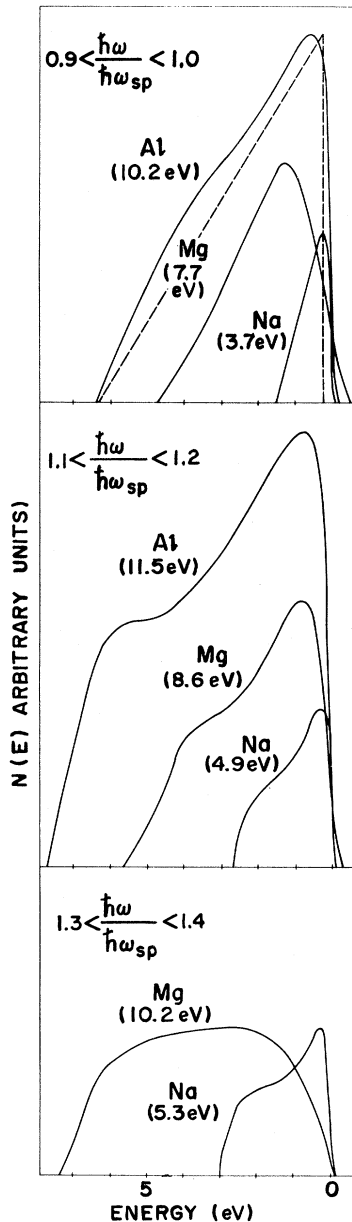


FIG. 12. Electron distribution curves (EDC's) for Al, Mg, and Na. The top frame is for excitation energies between 90% and 100% of the surface plasma energy $\hbar\omega_{sp}$, and EDC's show triangular shapes characteristic of EDC's in the surface-effect theory (dashed curve). The middle frame is for excitation energies 10% to 20% above the surface plasma energy, and the EDC's have low lying structure indicative of scattered electrons from volume photoexcitation. Secondary electrons begin to dominate the shapes of the EDC's in the bottom frame.

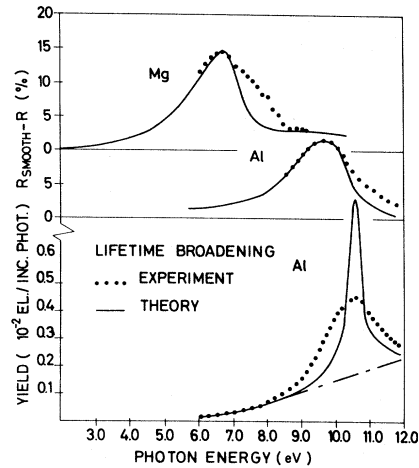


FIG. 13. Experimental and calculated lifetime-broadening effects. The solid curves for both the reflectance drops in Al and Mg (Refs. 11 and 18) and photoyield increase for Al (Ref. 11) were calculated from a volume-effect decay theory (Refs. 40 and 48). Experimental data are shown as dotted curves.

Coupling to plasmons, and thus this mode of exciting the surface effect on slightly roughened surfaces, should terminate at or just above the high- k surface plasma energy, and thus excitation of the surface effect should terminate near this energy for normally incident light. Since there is little possibility of the creation of secondary or scattered electrons in surface photoexcitation,⁴⁶ the termination of the surface effect would be expected to manifest itself as an emergence of low-energy electron peaks characteristic of scattered electrons in the volume theory.

The EDC's of Al,¹¹ Na,⁴⁷ and Mg¹⁸ shown in Fig. 12 indicate just such an effect. EDC's plotted for excitation energies (90–100)% of the high- k surface-wave energy in the top frame show no strong evidence for secondary or scattered electrons, and their triangular shape is in good agreement with the shape of the EDC calculated in the surface theory of this paper and shown as a dashed curve. At (10–20)% above the surface-wave cutoff energy in the middle frame, all three metals show the emergence of low-lying scattered electrons characteristic of the volume theory. In the bottom frame, secondary electron peaks begin to dominate the shapes of the curves, particularly in Mg, the least free-electron-like of the three metals.

2. Lifetime Broadening in Surface-Wave Decay

It was first suggested by Wilems and Ritchie²¹ that surface photoexcitation might contribute quite heavily to the lifetime broadening of high- k surface plasmons. However, in more recent calculations⁴⁰ it has been assumed that volume photoexcitation

dominates the broadening of the lower- k surface plasmons excited by optical radiation upon typical real surfaces. The result of the present calculation on Al is somewhat in contradiction to this recent view, indicating that the surface effect should dominate plasmon loss for all $k_{sp} \geq 5 \times 10^{-2} \text{ \AA}^{-1}$ (Fig. 7). Such surface waves are easily excited on real Al surfaces.¹¹

The experimental reflectance and photoyield curves for optically excited plasmons in Al¹¹ and Mg¹⁸ in Fig. 13, in fact show broadening of excited plasmons that is appreciably greater than predicted from just a volume-effect decay mechanism (solid curves).⁴⁸ The Al broadening near 10.5 eV was found to be about 2.5 times that expected from a pure volume theory. This value is reasonable and consistent with the calculations of this paper. Figure 7 indicates that 2.5 times volume-effect broadening should occur for plasmons with wave vectors $k_{sp} \approx 6 \times 10^{-2} \text{ \AA}^{-1}$ (easily excited on real surfaces). Also from the present calculation, one finds this particular surface wave should result in the surface-effect emission of ~ 0.16 electrons per decaying plasmon, in good agreement with the experimental observation of ~ 0.20 electrons per plasmon near 10.5 eV.

A related point of importance is that plasmon damping in the surface-effect theory would be expected to increase linearly in k in agreement with recent inelastic low-energy electron diffraction (LEED) observations in Al by Bagchi *et al.*⁴⁹ While their measurements showed appreciably weaker broadening than indicated in Fig. 13, the good agreement between the experimental broadening observed in Fig. 13 and the calculations of this paper tend to provide further strong evidence for the surface effect in plasmon decay.

B. Surface Photoelectric Effect in Alkali Metals

Perhaps the most intriguing question with regard to the surface photoelectric effect is the question of why the effect has not been experimentally observed in direct optical excitation. Virtually all attempts at this observation to date have been on the monovalent alkali metals.¹⁴⁻¹⁷ A certain explanation of why these attempts have failed is impossible, but we feel that we can at least give an explanation that is consistent with the picture developed in recent experiments^{11,47,50} and in the results of this paper. This explanation may be conveniently divided into two distinct spectral regions as shown in Smith and Spicer's⁴⁷ photoyield data on Na in Fig. 14.

At lower energies, the difficulty in obtaining smooth alkali films^{47,50} would be expected to introduce strong coupling to surface plasmons, consistent with observations in Al.¹¹ It is not surprising therefore that Smith's data show strong

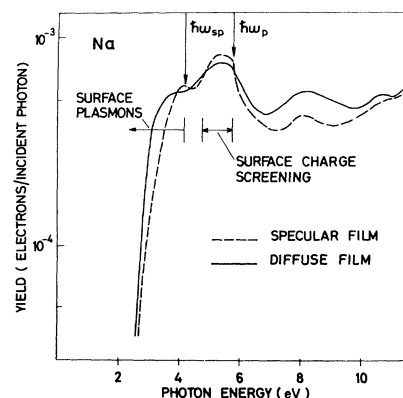


FIG. 14. Photoyield from diffuse and specularly reflecting Na films (Ref. 47). The data conveniently divide into a spectral region below $\hbar\omega_{sp}$, for which coupling to surface waves is appreciable, and a spectral region near $\hbar\omega_p$, where surface charge effects cause a suppression of the surface effect.

coupling to surface waves on the specular film prepared on a liquid-N₂-cooled substrate (note the sharp peak right at $\hbar\omega_{sp}$), as well as on the diffusely reflecting film prepared at room temperature. It has been observed more recently that this coupling is enhanced by the peculiar susceptibility of the alkalis to surface contamination.⁵⁰ In this region below the high- k surface plasma energy, it is likely that surface-wave decay dominates the photoyield even in the smoothest films prepared, and with $\hbar\omega_{sp}$ so close to threshold in the monovalent alkalis, it likely dominates right down to threshold. Most attempts to optically excite the surface effect in the alkalis have involved measurements of the vector ratio of yields as described in Sec. III C. In principle, p -polarized light should give an anomalously large yield indicative of surface-effect excitation. In reality, however, we see that measurements of the vector ratio in this energy range, instead of giving a measure of the ratio of volume-effect to surface-effect emission, will merely give the ratio of *coupling* to surface waves for s -polarized vs p -polarized optical excitation. Essentially, the strong surface effect inherent in plasmon decay has been the very mechanism that has served to obscure and confuse previous attempts to optically excite and observe the surface effect at low energies in the alkalis.

At higher energies approaching $\hbar\omega_p$, we have seen that surface charge-screening effects cause a strong suppression of the surface effect. Although spurious excitation of surface plasmons is no longer a problem, it is doubtful that the surface effect is strong enough to be observed in this energy range. Smith's failure to observe a higher photoyield in his rough film than in his specular film

over these energies tends to substantiate this conclusion. Above the volume plasma energy our calculations on Al have indicated that the surface effect should increase somewhat. However, these Al calculations assumed that Al is well described in the Drude picture at these energies with ϵ_2 monotonically decreasing with energy. In fact, it is known from recent experiments⁵¹ that ϵ_2 increases in the alkalis above $\hbar\omega_p$, so that the ratio of surface-to-volume photoemission would be expected to be less in the alkalis than in Al. Problems of observing the surface effect in this spectral range are compounded by experimental problems of obtaining polarizers and preparing opaque films. A more certain analysis of the surface effect in the alkalis should await improved calculations of the effect such as described for Al in this paper.

V. SUMMARY AND CONCLUSIONS

A modified form of the Mitchell-Makinson^{2,4} time-dependent perturbative calculation of the surface photoelectric effect has been presented, and numerical results have been calculated for Al. Modifications include the calculation of electron excitation back into the metal as well as electron emission into vacuum. A significant improvement in the treatment of surface fields and surface-polarization charge variations is based on the Bloch hydrodynamic equations. This approach allows calculation of the surface effect to the volume plasma energy ($\hbar\omega_p$) and beyond.

It is argued on the basis of recent experiments that atomically smooth and clean metallic surfaces may be reliably obtained. The assumption of such ideally smooth surfaces allows a generalized calculation of the surface photoelectric effect in terms of p -polarized-light excitation at arbitrary oblique angles of incidence. For sufficiently smooth surfaces, optical coupling to the surface effect by p -polarized light is considered direct. Where roughness-induced coupling to surface waves (plasmons) is significant, the plasmon mode of surface-effect excitation is treated as a special case of p -polarized-light excitation at an appropriate complex angle of incidence. The general expressions for surface photoexcitation by p -polarized light are shown to be factorable into *excitation field factors* dependent upon optical constants and angle of incidence, and factors termed *characteristic photoexcitation*, dependent upon the details of the surface barrier and surface-polarization charge variations, but independent of angle of light incidence.

Numerical evaluation of the characteristic photoexcitation factors indicates an enhancement in the surface effect at energies well below $\hbar\omega_p$, associated with electronic interaction with surface-polarization charge. For energies near $\hbar\omega_p$, sur-

face charge screening of excitation fields is seen to introduce a correspondingly strong suppression of the surface effect. Surface excitation necessarily requires an excitation field component normal to the surface, and this dependence is seen explicitly in the strong dependence of the excitation field factors upon angle of p -polarized-light incidence. The large magnitude of the field factors at complex angles of incidence characteristic of surface-wave (plasmon) excitation of the surface effect indicates that surface plasmons are a uniquely effective mode of p -polarized-light excitation of the surface photoelectric effect.

Comparisons of the relative strengths of calculated surface photoexcitation and volume photoexcitation have been carried out, with an isotropic volume-effect photoexcitation model used where appropriate.

The results indicate that the surface effect is sufficiently strong at energies well below $\hbar\omega_p$ to dominate the decay of high- k surface plasmons typically excited on real surfaces, and to dominate the photoemission associated with these decaying plasmons for all plasmon wave vectors and energies. The effect is somewhat weaker in direct optical excitation, but is still sufficiently strong so that the surface effect dominates photoemission from p -polarized-light excitation at high real angles of incidence over a broad energy range below $\hbar\omega_p$. The effect in fact becomes exceedingly strong at energies approaching threshold in polyvalent Al, with the predicted ratio of photoyield from p - vs s -polarized light many times the ratio expected in a pure volume theory. This high calculated ratio implies that the measurement of s - and p -polarized light photoyield ratios at threshold energies in nearly-free-electron polyvalent metals should provide a uniquely effective means of observing the heretofore unobserved direct optical excitation of the surface photoelectric effect.

As one moves to higher energies, the ratio of surface-to-volume effect photoemission for high real angles of incidence is found to be much less, becoming almost completely suppressed near $\hbar\omega_p$ and remaining relatively weak even above the volume plasma energy.

The importance of surface roughness in promoting coupling to surface photoexcitation is examined by calculating the surface-to-volume effect ratio for an angle of incidence believed to be comparable to the surface angle presented to normally incident light by typical smooth surfaces. The ratio is found to be negligible for all but the lowest excitation energies. This result tends to confirm that normal incidence excitation of smooth surfaces should be regarded as inducing a volume photoeffect in all but the most nearly-free-electron metals, and even in these metals, the surface effect

for normal incidence light should be considered significant only at energies near threshold, or at energies where coupling to surface plasmons is appreciable.

Direct results and implications of these surface-effect calculations have been compared to existing experimental data. Comparisons divide conveniently into discussions of the surface-wave (plasmon) vs direct optical modes of p -polarized-light excitation of the surface photoelectric effect.

The surface-plasmon mode is predicted to be the strongest mode of surface-effect excitation and it is pointed out that surface-plasmon-decay data provide the only strong experimental evidence to date for the surface photoelectric effect. Plasmon-induced yield increases and observed surface-plasmon broadening in Al¹¹ are shown to be in good quantitative agreement with the calculation, while EDC's taken on Al,¹¹ Mg,¹⁸ and Na⁴⁷ are shown to be in qualitative agreement with the picture developed in the calculation.

The historical inability to observe the surface effect in direct optical excitation of the alkalis¹⁴⁻¹⁷ is examined and explained in terms of the results of the calculation. Spurious coupling to the strong surface effect associated with surface-plasmon excitation is thought to be responsible for the inability to obtain unambiguous data at low energies in the alkalis. At higher energies near and above $\hbar\omega_p$, it is thought that the strong surface charge screening effects described in this paper cause a suppression of the surface effect to where it is not easily observed. Clearly, direct optical excitation of the

surface effect is most easily observed at low energies, and it is thought that such observations will be least susceptible to spurious surface-wave coupling if in the future one looks at polyvalent metals such as Al where threshold energies lie well below the surface plasma energy.

In summary, this paper describes a general calculation of the surface photoelectric effect which is equally applicable to surface-wave (plasmon) or direct optical excitation. The calculation is based on an improved treatment of surface-polarization charge-density variations. Results indicate a suppression of the surface effect near and above the volume plasma energy and an enhancement at lower energies. Both the surface-wave and optical modes of surface-effect excitation are strong in this low-energy region, but the surface-wave (plasmon) mode of excitation is found to be particularly effective, in agreement with recent experiments. Previous failures to observe direct optical excitation of the surface effect are explained, and it is suggested that such future observations would be best made near threshold energies in polyvalent nearly-free-electron metals such as Al.

ACKNOWLEDGMENTS

The author would like to express his deep gratitude to Professor S. Hagström and Professor W. E. Spicer for their encouragement in this work, and to Professor K. F. Bergren for several helpful suggestions. Useful discussions with Dr. R. H. Ritchie, Dr. W. L. Schaich, and Professor N. W. Ashcroft are also gratefully acknowledged.

*Present address: RCA David Sarnoff Research Center, Princeton, N.J. 08540.

¹K. Mitchell, Proc. R. Soc. A **146**, 442 (1934).

²K. Mitchell, Proc. Camb. Philos. Soc. **31**, 416 (1935).

³K. Mitchell, Proc. R. Soc. A **153**, 513 (1936).

⁴R. E. B. Makinson, Proc. R. Soc. A **162**, 367 (1937).

⁵I. Adawi, Phys. Rev. A **134**, 788 (1964).

⁶W. L. Schaich and N. W. Ashcroft, Phys. Rev. B **3**, 2452 (1971).

⁷J. Crowell and R. H. Ritchie, J. Opt. Soc. Am. **60**, 794 (1970).

⁸A. R. Melnyk and M. J. Harrison, Phys. Rev. B **2**, 835 (1970), and Phys. Rev. B **2**, 851 (1970).

⁹M. L. Théye, Phys. Rev. B **2**, 3060 (1970).

¹⁰H. Kanter, Phys. Rev. B **1**, 522 (1970).

¹¹J. G. Endriz and W. E. Spicer, Phys. Rev. B **4**, 4159 (1971).

¹²J. A. Stratton, *Electromagnetic Theory* (McGraw-Hill, New York, 1941).

¹³J. G. Endriz and W. E. Spicer, Phys. Rev. Lett. **27**, 570 (1971).

¹⁴H. Mayer and H. Thomas, Z. Phys. **147**, 419 (1957).

¹⁵S. Methfessel, Z. Phys. **147**, 442 (1957).

¹⁶G. A. Boutry, *et al.*, C.R. Acad. Sci. (Paris) **261**, 383 (1965).

¹⁷M. Brauer, Phys. Status Solidi **14**, 413 (1966).

¹⁸T. F. Gesell and E. T. Arakawa, Oak Ridge National Laboratory Report No. ORNL-TM-2617, 1971 (unpublished).

¹⁹G. D. Mahan, Phys. Rev. B **2**, 4334 (1970).

²⁰Whittaker and Watson, *Modern Analysis* (Cambridge, London, 1935), Chap. XVI.

²¹R. E. Wilems and R. H. Ritchie, Oak Ridge National Laboratory Report No. ORNL-TM-2101, 1968 (unpublished).

²²L. Landau, J. Phys. USSR **10**, 25 (1946).

²³L. I. Schiff and L. H. Thomas, Phys. Rev. **47**, 860 (1935).

²⁴The shape of the field component a_z remains independent of angle of incidence for complex angles characteristic of most surface waves (plasmons). Only for very high- k surface waves, does the shape of a_z become a function of k (angle), see Ref. 7.

²⁵Care must be taken to avoid Mitchell's error (Refs. 1 and 2) in the assumed electron density in k space, see Ref. 4.

²⁶In the notation of Mitchell (Ref. 2) used in this paper, a positive going wave in direction k is given by $e^{-ik \cdot r}$ with implied time variation $e^{i\omega t}$, in contrast with the usual convention $e^{-i\omega t}$. Electromagnetic field parameters such as ϵ , Γ , have thus been defined in a manner consistent with this time variation.

²⁷Much of the notation of this paper follows the convenient complex form of Fresnel's equations for p -polarized light found in T. S. Moss, *Optical Properties of Semiconductors* (Academic, London, 1959). These equations imply that the complex angle of incidence defined in Eq. (19) will yield incident and refracted waves which decay away from the surface. The reflected wave grows away from the surface, and the criteria on $\phi_{sp}(\omega)$ that the reflection coefficient be zero leads to Eqs. (20), (21), and surface waves.

²⁸D. M. Newns, Phys. Rev. B **1**, 3304 (1970).

²⁹Polarization-charge-density attenuation lengths for Al given by Eq. (23) range from a minimum value $\Gamma_{\text{real}}^{-1}(0) \approx 0.7 \text{ \AA}$ to a maximum value $\Gamma_{\text{real}}^{-1}(\gamma_p) \approx 2.6 \text{ \AA}$.

³⁰It is assumed τ^{-1} is the same scattering rate as used in the Drude model fit to Al-reflectance data in B. P. Feuerbacher and W. Steinman, *Opt. Commun.* **1**, 81 (1969). (See Table I.)

³¹F. Sauter, *Z. Phys.* **203**, 488 (1967).

³²I. Lindau and P. O. Nilsson, *Phys. Lett. A* **31**, 352 (1970).

³³M. Anderegg, B. Feuerbacher, and B. Fitton, *Phys. Rev. Lett.* **27**, 1565 (1971).

³⁴R. H. Ritchie and R. E. Wilems, *Phys. Rev.* **178**, 372 (1969).

³⁵Wavefunctions in the region of the image-charge potential were determined from a Runge-Kutta solution of the wave equation.

³⁶G. Hass and J. E. Waylonis, *J. Opt. Soc. Am.* **51**, 719 (1961).

³⁷J. G. Endriz and W. E. Spicer, *Phys. Rev. B* **4**, 4144 (1971).

³⁸F. Wooten, T. Huen, and R. N. Stuart, in *Optical Properties and Electronic Structure of Metals and Alloys*, edited by F. Abeles (North-Holland, Amsterdam, 1966), p. 332.

³⁹T. F. Gesell and E. T. Arakawa, *Phys. Rev. Lett.* **26**, 377 (1971).

⁴⁰J. M. Elson and R. H. Ritchie, *Phys. Rev. B* **4**, 4129 (1971).

⁴¹This term has been used extensively in the literature, e.g., R. M. Broudy, *Phys. Rev. B* **3**, 3641 (1971).

⁴²C. N. Berglund and W. E. Spicer, *Phys. Rev.* **136**, A1030 (1964).

⁴³This paper concludes that the surface effect is most easily optically detected at energies well below $\hbar\omega_p$ where both *s*- and *p*-polarized light are refracted nearly normal to the surface, even for quite high angles of incidence. Light polarization dependence in the photoyield associated with photoexcitation directionality effects (Ref. 19) should thus be strongly subdued at these energies.

⁴⁴A similar method was used to detect surface-plasmon excitation of the surface effect (Refs. 11 and 13). Excitation was reliably calculated in the volume theory and experimental deviations assigned to the surface effect.

⁴⁵This volume effect calculation, $(S_p/V_p)Y_{CH:volume} = \frac{1}{2} \alpha(\phi)V_e(\hbar\omega)y(\hbar\omega)$ corresponds to the lowest-lying volume-effect curve in Fig. 2, Ref. 13. The volume-effect calculations of that reference were based on experimentally observed photoyield, and thus differ from the analytically defined isotropic-excitation model of the present calculation.

⁴⁶Surface-excited electrons emitted into vacuum necessarily escape before they can interact with other electrons. Surface back excited electrons may inelastically scatter back into vacuum, but this process should have a rather low probability.

⁴⁷N. V. Smith and W. E. Spicer, *Phys. Rev.* **188**, 593 (1969).

⁴⁸Lifetime broadening for Al was calculated from the volume decay theory of Ref. 40 and the optical constants of Table I. The calculated broadening for the reflectance curves of Fig. 13 include effects of coupling to plasmons of different energies as well as lifetime broadening. The photoyield calculation is broadened only by lifetime effects.

⁴⁹A. Bagchi, C. B. Duke, and P. J. Feibelman, *Phys. Rev. Lett.* **27**, 998 (1971).

⁵⁰R. J. Whitefield and J. J. Brady, *Phys. Rev. Lett.* **26**, 380 (1971).

⁵¹J. C. Sutherland, R. N. Hamm, and E. T. Arakawa, *J. Opt. Soc. Am.* **59**, 1581 (1969); U. S. Whang, E. T. Arakawa, and T. A. Callcott, *Phys. Rev. Lett.* **25**, 646 (1970).

Resonant Raman Scattering from $\text{Al}_x\text{Ga}_{1-x}\text{As}$

Jagdeep Shah, A. E. DiGiovanni, T. C. Damen, and B. I. Miller

Bell Telephone Laboratories, Holmdel, New Jersey 07733

(Received 11 September 1972)

We report the results of a detailed study of resonant Raman scattering from the mixed crystal $\text{Al}_x\text{Ga}_{1-x}\text{As}$ at 2 °K using a continuously tunable dye laser. The dye laser enables us to obtain the exact resonance line shape. Comparison of the resonance behavior of the GaAs-like and the AlAs-like LO phonons allows us to determine the energy of the band gap accurately. In addition to the resonance behavior, we have also studied the 1-LO linewidths and line shapes, the behavior of the TO phonon and local modes, and also certain broad luminescence features present in the spectra.

I. INTRODUCTION

Resonant Raman scattering from solids has been investigated rather extensively in the last few years from experimental and theoretical viewpoints.¹ Most of the experimental work until now has been done by using the various discrete lines of different lasers,¹ by varying temperature² of the sample, or by applying external perturbations such as magnetic field³ or stress⁴ on the sample. However, the recent advent of pulsed⁵ and cw⁶ dye lasers provides a very powerful tool for studying the resonance phenomena in Raman scattering from solids. For example, the use of a flashlamp-pumped dye laser enabled us to study in detail the resonant Raman scattering due to bound excitons in CdS.⁷

A cw dye laser has been recently used by Cerdeira *et al.*⁸ for studying resonance phenomena in germanium.

In this paper we describe our results on resonant Raman scattering from $\text{Al}_x\text{Ga}_{1-x}\text{As}$ by using a cw dye laser. We can obtain the exact line shape of resonance by using this technique. Furthermore, this technique enables us to compare the resonance behavior of two different LO phonons (one GaAs-like, another AlAs-like) and provides us with a technique for obtaining the band gap of the material rather accurately. ("GaAs-like" LO phonon is the one whose energy approaches that of the LO phonon in GaAs as *x* approaches zero.)

It should be mentioned here that GaAs is a direct-gap ($E_g \approx 1.52$ eV at 2 °K) material, whereas

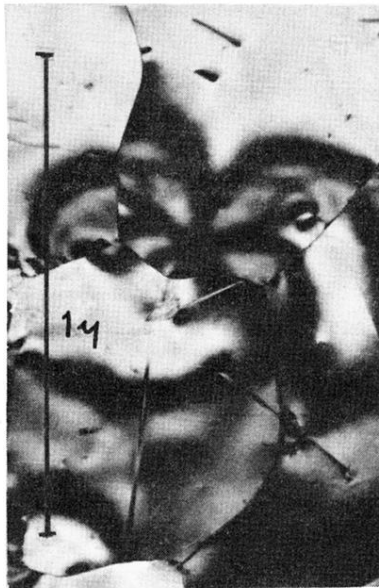


FIG. 1. Transmission electron micrograph of a 158- \AA -thick vacuum-evaporated film of Au. Note that the lateral dimensions of the crystals are comparable to $1\ \mu$ (M. L. Théye, Ref. 9).